

Sporogenesis, gametogenesis and pollen morphology of *Solanum japonense* and *S. septemlobum* (Solanaceae)

Yanshuang Liu, Lei Gu and Jiaxi Liu*

College of Life Sciences, Capital Normal University, Beijing, China

*Corresponding author: liu-jiaxi@263.net

Received: July 24, 2017; Revised: October 20, 2017; Accepted: November 9, 2017; Published online: November 22, 2017

Abstract: *Solanum japonense* Nakai and *S. septemlobum* Bunge are medicinal plants used chaotically in traditional Chinese medicine because they have the same Chinese name, Shuyangquan. In this study, anther wall development, microsporogenesis, male gametophyte development, megasporogenesis and female gametophyte development of *S. japonense* and *S. septemlobum* were studied using traditional paraffin section technology for the first time, and their pollen morphologies were compared using scanning electron microscopy. The results showed that both species exhibit dicotyledonous anther wall development, dual tapetum origination, secretory tapetum development, simultaneous microsporocyte cytokinesis, tetrahedral tetrad, coexistent 2-celled and 3-celled mature spheroidal pollen grains that are circular along the equatorial view and have tricolporate grooves, 2 locules per ovary, axial placenta, anatropous, unitegmic and tenuinucellate ovule, linear megaspore tetrad, as well as monosporic Polygonum type of embryo sac, where the chalazal megaspore develops into the functional megaspore and the other three megaspores degenerate. However, the pollen grains of *S. japonense* are circular along the polar view, while those of *S. septemlobum* are triangular; the pollen surface ornamentation of *S. japonense* is granulate-verrucate-punctate, while that of *S. septemlobum* is granulate-punctate-fossula. These results enrich the embryological data of *Solanum* and provide palynological bases for the classification of these two species.

Key words: *S. japonense*; *S. septemlobum*; embryonic development; pollen morphology; taxonomy

INTRODUCTION

Solanum belongs to the family Solanaceae [1] and is the largest genus in the family [2]. It comprises approximately 1200 species, of which 41 are found in China [3]. Plants in *Solanum* have very high economic values. In addition to food, they are also used as ornamental [4] and medicinal plants [5,6].

S. japonense Nakai is a medicinal plant of the section *Dulcamara* of the genus [7]. It is used to disperse pathogenic wind, invigorate blood circulation and relieve rheumatism, joint pain and dizziness [8]. *S. septemlobum* Bunge is commonly classified into section *Polybotryon* of the genus [7], but it was classified into subgenus *Potatoe* by D'Arcy [9]. *S. septemlobum* contains some pharmaceutically active substances, which can inhibit tumor cell growth [10,11], and it is often used as an antipyretic [12].

As medicinal plants, *S. japonense* and *S. septemlobum* are easily misidentified. Both have been used as

an ingredient of Shuyangquan, a traditional Chinese medicine (TCM) [13,14]. Correct identification of medicinal plants is of great significance for the development and application of TCM [15]. *S. japonense* and *S. septemlobum* plants are usually determined by their plant morphology and medical properties [16]. Their embryology has not been sufficiently studied. Previous embryological studies on *Solanum* were mainly focused on the development of embryo and endosperm [17-20] or ultrastructures during embryonic development [21-26].

Luo and Zhou [27] studied the pollen morphology of *S. japonense* using light microscopy and scanning electron microscopy (SEM), but the SEM only provided the equatorial view. Wang et al. [28] studied the pollen morphology of *S. septemlobum* using light microscopy, but without showing the micrographs of pollen grains. Du et al. [29] studied in detail pollen morphology of *S. septemlobum* using SEM.

In this paper, we studied anther wall development, microsporogenesis, male gametophyte development, megasporogenesis and female gametophyte development of *S. japonense* and *S. septemlobum* for the first time, with the aim of enriching the embryological data about *Solanum*. Our work is an attempt toward a better understanding of the taxonomic relationships of these two species using palynological characteristics.

MATERIALS AND METHODS

Experimental material

Flower buds and fruits of *S. japonense* and *S. septemlobum* at different developmental stages were collected in 2014 from Beijing Songshan of Yanqing County, Beijing, and Hohhot, Inner Mongolia, China. Voucher samples are stored in the Herbarium of the Institute of College of Life Sciences, Capital Normal University (CNU, *S. japonense* Voucher No. 14021, *S. septemlobum* Voucher No. 14025).

Methods

The flower buds and fruits at different maturity stages were fixed in formalin-acetic acid-alcohol (FAA) and

stored at 4°C. Materials were dehydrated through tertiary butyl alcohol series and embedded in paraffin wax. Sections, cut between 5–6 µm thickness, were stained in modified hematoxylin [30]. Mature pollen grains were placed on aluminum stubs with double-sided adhesive tapes. All the samples were coated with gold-palladium and were viewed under a Hitachi S-4800 scanning electron microscope. In addition, the polar axis (P) × equatorial axis (E) of 20 pollen grains from each species were measured and the size of pollen grains was expressed as the average P×E. Pollen size was classified based on their longest diameter and the shape was defined using P/E as described by Erdtman [31]. Palynological terminology used is according to Wang et al. [28] and Punt et al. [32].

RESULTS AND DISCUSSION

Plant morphology

Inflorescences of both *S. japonense* and *S. septemlobum* are conical, bearing flowers with purple corolla and green spots on the base, reflexed petals, yellow, oblong, basal anthers and green capitate stigma located higher than the anthers (Fig. 1A, Fig. 2A-B). In addition, *S. japonense* has a long, acuminate leaf apex

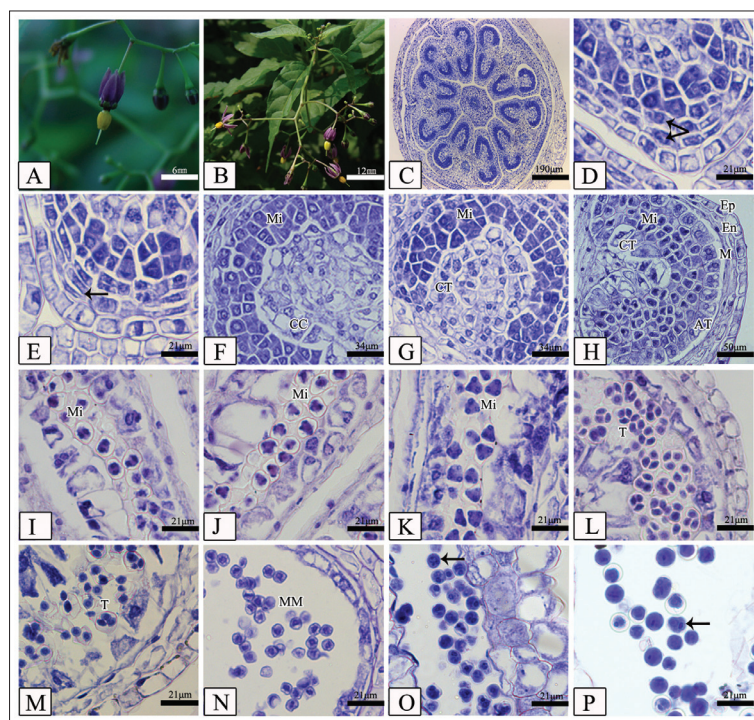


Fig. 1. Plant morphology, microsporogenesis and male gametophyte development of *Solanum japonense*. **A** – Flowers. **B** – Inflorescence and leaf blades. **C** – Cross-section of bud, showing 5 anthers with 4 microsporangia each. **D-E** – Partial cross section of anther, showing differentiated anther wall (arrows). **F** – Cross section of anther, showing microsporocytes and connective cells. **G** – Cross section of anther, showing connective tapetum. **H** – Cross section of anther, showing connective tapetum and anther tapetum. **I** – Microsporocytes at meiosis telophase I. **J** – Microsporocytes at meiosis anaphase II. **K** – Microsporocytes at meiosis telophase II. **L** – Tetrahedral tetrad. **M** – Disintegrated tetrad. **N** – Mononucleate microspores. **O** – Mitosis of microspores, showing 2-celled and 3-celled pollen grains (arrow) and separation of germ cells and vegetative cells by arc cell walls. **P** – Mature pollen grains and fusiform germ cells (arrow). AT – anther tapetum; CC – connective cells; CT – connective tapetum; En – endothecium; Ep – epidermis; M – middle layer; Mi – microsporocytes; MM – mononucleate microspores; T – tetrad.

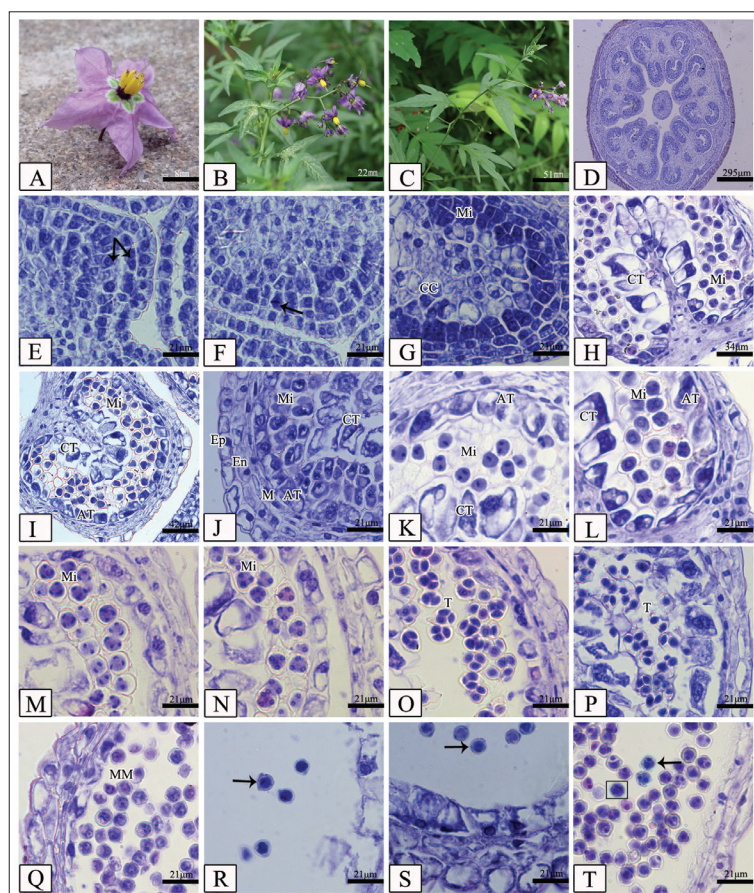


Fig. 2. Plant morphology, microsporogenesis and male gametophyte development of *Solanum septemlobum*. A – Flower. B – Inflorescence. C – Leaf blades. D – Cross section of bud. E-F – Differentiated anther wall (arrows). G – Microsporocytes and connective cells. H – Cross section of anther, showing connective tapetum. I – Cross section of anther, showing connective tapetum and anther tapetum. J – Microsporocytes at zygotene stage of meiosis prophase I. K – Microsporocytes at meiosis anaphase I. L – Microsporocytes at meiosis telophase I. M – Microsporocytes at meiosis anaphase II. N – Microsporocytes at meiosis telophase II. O – Tetrahedral tetrad. P – Disintegrated tetrahedral tetrad. Q – Microspore at the mononuclear stage. R – Microspores at metaphase of mitosis (arrow). S – Microspores at anaphase of mitosis (arrow). T – Fusiform germ cells (block) as well as 2-celled and 3-celled (arrow) mature pollen grains. AT – anther tapetum; CC – connective cells; CT – connective tapetum; En – endothecium; Ep – epidermis; M – middle layer; Mi – microsporocytes; MM – mononucleate microspores; T – tetrad.

with undulate margin (Fig. 1B), while *S. septemlobum* has upper leaf blades with nearly entire margin, an obtuse apex and 3-lobed or 5-lobed lower leaf blades (Fig. 2C).

Anther wall development

Both *S. japonense* and *S. septemlobum* have 5 anthers containing 4 microsporangia each (Fig. 1C, Fig. 2D). Almost all species of *Solanum* have 5 anthers per flower [7], except *S. procumbens* Loureiro, and *S. tuberosum* Linnaeus, which have 4 and 6 anthers per flower, respectively [7,33]. The primary wall cells of both species undergo periclinal division, forming an outer layer and an inner layer. At this period, the anther wall contains a total of three layers: an outer layer, inner layer and epidermis (Fig. 1D, Fig. 2E). The outer layer cells undergo another division, forming the endothecium and the middle layers. The inner layer cells directly develop into anther tapetum (Fig. 1E, Fig. 2F). The completely differentiated anther wall

comprises the epidermis, endothecium, middle layer and tapetum (Fig. 1H, Fig. 2J). The anther wall development is of dicotyledonous type (Table 1). Anther wall development of Angiospermae is classified as basic type, dicotyledonous type, monocotyledonous type and reduced type [34]. García [35] studied the anther wall development of 32 species of *Solanum* and found both basic type and dicotyledonous type. Bhandari and Sharma [21] also found both basic type and dicotyledonous type in *S. nigrum* Linnaeus.

At the microsporocyte stage, the connective cells protrude into the microsporangium (Fig. 1F) and some of them begin to differentiate. Those with a slightly larger nucleus and nucleolus further develop into the connective tapetum (Fig. 1G, Fig. 2G). During development of the anther, anther tapetum and connective tapetum, different morphological features are displayed. Overall, the tapetum is heterotypic (Fig. 1H, Fig. 2H-I) and has a dimorphic development. A previous report also showed that *S. tuberosum* has a heterotypic tapetum, but did not describe its detailed

Table 1. The embryological and palynological characteristics of *Solanum japonense* and *Solanum septemlobum*

	<i>Solanum japonense</i>	<i>Solanum septemlobum</i>
Embryological characteristics		
Microsporangia	4	4
Anther wall	Dicotyledonous	Dicotyledonous
Tapetum origination	Dual	Dual
Tapetum	Secretory	Secretory
Cytokinesis	Simultaneous	Simultaneous
Microspore tetrads	Tetrahedral	Tetrahedral
Mature pollen	2-celled, 3-celled	2-celled, 3-celled
Ovary	2 locules	2 locules
Placenta type	Axial	Axial
Ovule	Anatropous	Anatropous
Integument	Unitegmic	Unitegmic
Nucellus	Tenuinucellate	Tenuinucellate
Megaspore tetrads	Linear	Linear
Embryo sac	Polygonum type	Polygonum type
Palynological characteristics		
Size (µm)	8.5 (7.4-9.8) × 8.9 (7.4-10.5)	8.8 (7.6-9.8) × 9.2 (7.9-10.7)
Size class	Small	Small
Shape	Spheroidal	Spheroidal
Polar view	Circular	Triangle
Equatorial view	Circular	Circular
Aperture	Tricolporate	Tricolporate
Surface ornamentation	Granulate-verrucate-punctate	Granulate-punctate-fossula

developmental process [36]. In addition, a heterotypic tapetum has also been found in *Lycium* and *Capsicum annuum* L. belonging to Solanaceae [37-39].

At prophase I of the meiosis, the tapetum is well developed (Fig. 1H, Fig. 2J). Afterwards, tapetal cells separate from each other, deform, and gradually disintegrate at their original position (Fig. 1I, Fig. 2K). At the early microspore stage, tapetal cells further disintegrate (Fig. 1N) and completely disappear in the fully mature pollen grains. The tapetum development is of the secretory type (Table 1).

Microsporogenesis

Microsporocytes at the initial stage are composed of large cells with a dense cytoplasm, prominent nucleus, multiple nucleoli and no obvious vacuole (Fig. 1F, Fig. 2G). The cells undergo meiosis. At prophase I, the chromatin undergoes long-term, complex changes and gradually concentrates to thicker and shorter chromosomes, the nucleoli disintegrate and the nuclear membranes disappear. Prophase I includes five stages, leptotene (Fig. 1H), zygotene (Fig. 2J), pachytene,

diplotene and diakinesis. At meiosis metaphase I, the paired homologous chromosomes are arranged on the equatorial plate at the cell center. At meiosis anaphase I, homologous chromosomes gradually separate from each other under the traction of spindle fibers, moving toward the two cell poles (Fig. 2K). At meiosis telophase I, chromosomes at the two poles gather together again, forming a new nuclear membrane and nucleolus (Fig. 1I, Fig. 2L), but not the cell wall. Thus, after meiosis I, no dyad appears.

The two daughter cells simultaneously undergo meiosis II. At meiosis anaphase II, the sister chromatids move towards the poles under the traction of the spindle fibers (Fig. 1J, Fig. 2M). At meiosis telophase II, the nuclear membrane reforms at the poles around the chromosomes and the two daughter cells undergo cytokinesis (Fig. 1K, Fig. 2N), forming a tetrahedral tetrad (Fig. 1L, Fig. 2O), like many other species of Solanaceae [40-43]. However, Tang et al. [44] found that *S. melongena* Linnaeus has both a tetrahedral and symmetrical tetrad. The microsporocytes cytokinesis of both *S. japonense* and *S. septemlobum* is of the simultaneous type (Table 1).

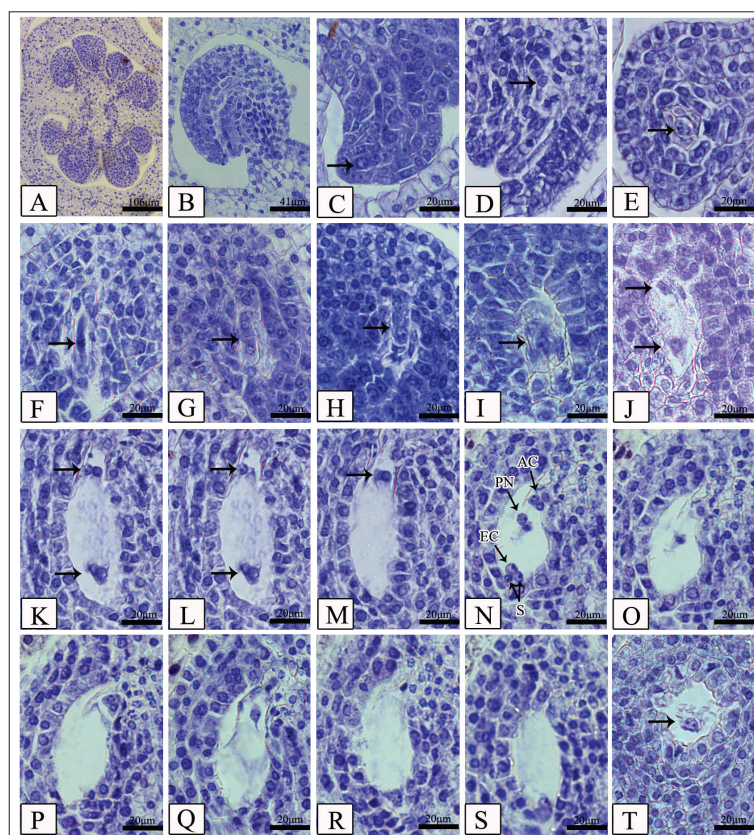


Fig. 3. Megasporogenesis and female gametophyte development of *Solanum japonense*. **A** – Cross-section of ovary. **B** – Anatropous ovules. **C** – Archesporial cells (arrow). **D** – Megasporocytes (arrow) at leptotene of meiosis prophase I. **E** – Megasporocytes (arrow) at diakinesis of meiosis prophase I. **F** – Megasporocytes (arrow) at meiosis metaphase I. **G** – Dyad (arrow). **H** – Linear tetrad (arrow). **I** – Mononuclear embryo sac (arrow). **J** – Binuclear embryo sac (arrows point to the nuclei). **K-M** – Tetranuclear embryo sac (arrows point to the nuclei) (K is pieced together by L-M, which are consecutive sections of the same embryo sac). **N-S** – 8-nucleate embryo sac (arrows) (N is pieced together by O-S, which are consecutive sections of the same embryo sac). **T** – Central cell fusion (arrow). AC – antipodal cells; EC – egg cell; PN – polar nuclei; S – synergids.

Male gametophyte development

With the dissolution of the callose wall, the tetrad gradually disintegrates (Fig. 1M, Fig. 2P) to free microspores. Furthermore, a distinct wall forms in the early microspores released from the tetrad (Fig. 1N). Meanwhile, these microspores rapidly enlarge in volume, and vacuoles occur in the cytoplasm, gradually forming a large central vacuole, which pushes the nuclei to one side of the cells. The cells are at the mononuclear stage (Fig. 2Q). At this time, microspores undergo mitosis (Fig. 2R-S), forming a larger vegetative cell and a smaller germ cell. The newly formed germ cell is close to the pollen wall and separated from the vegetative cells by an arch cell wall (Fig. 2T). Subsequently, the cell wall between the two cells disintegrates and the germ cell is detached from the pollen wall and free in the cytoplasm of the vegetative cell (Fig. 2T). Afterwards, germ cells in some pollen grains undergo further mitosis, forming two sperm cells (Fig. 1O, Fig. 2T). These sperm cells gradually change from spherical to oblong shape (Fig. 1P, Fig. 2T). The mature pollen grains of both *S. japonense*

and *S. septemlobum* are 2-celled and 3-celled (Fig. 1O, Fig. 2T). In previous studies, Dnyansagar and Cooper [17] found that the mature pollen grains of *S. phureja* Juzepczuk & Bukasov are both 2-celled and 3-celled, while Fukuda [41] found that the mature pollen grains of *S. tuberosum* are 2-celled.

Megasporogenesis

The gynoecium is bicarpellary, syncarpous, bilocular and has many ovules on axile placentation. However, Zhang et al. [3] believed that the ovary of *Solanum* has 2-5 locules. The ovules are anatropous, unitegmic and tenuinucellate (Fig. 3A-B, Fig. 4A-B), which is in agreement with the finding of Govil [45] that *Solanum tuberosum* var. Jyoti Gola has both anatropous and semi-anatropous ovules.

The megasporocyte directly develops from the archesporial cells under the nucellar epidermis and contains a dense cytoplasm and a prominent nucleus (Fig. 3C, Fig. 4C). During meiotic prophase I, the megasporocyte undergoes five phases: leptotene, zy-

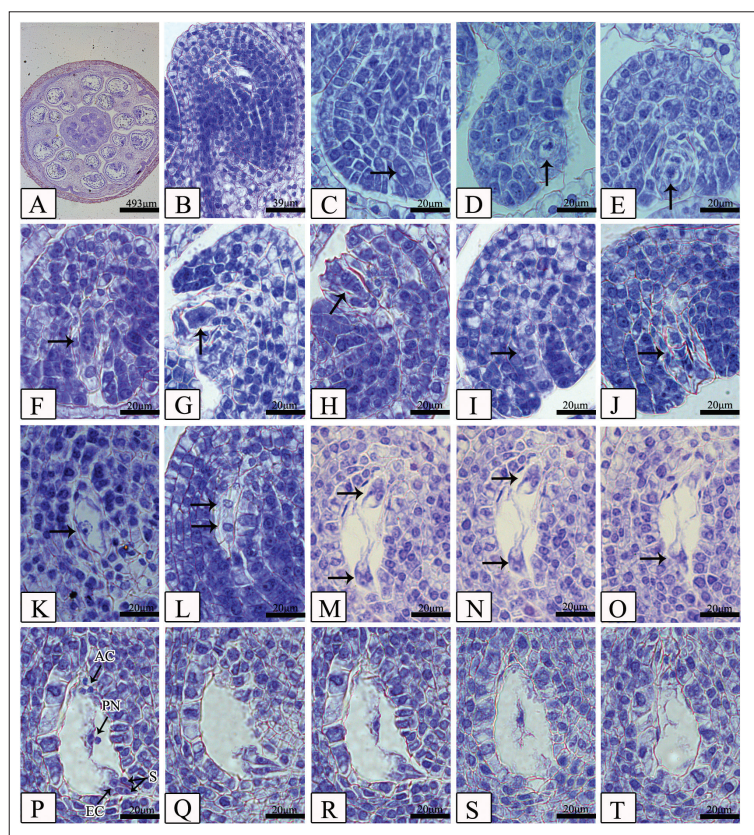


Fig. 4. Megasporogenesis and female gametophyte development of *Solanum septemlobum*. **A** – Cross-section of flower bud. **B** – Anotropous ovules. **C** – Archesporial cells (arrow). **D** – Megasporocytes (arrow) at leptotene of meiosis prophase I. **E** – Megasporocytes (arrow) at zygotene of meiosis prophase I. **F** – Megasporocytes (arrow) at diakinesis of meiosis prophase I. **G** – Megasporocytes (arrow) at meiosis metaphase I. **H** – Dyad (arrow). **I-J** – Tetrad (arrow). **K** – Mononuclear embryo sac (arrow). **L** – Binuclear embryo sac (arrows point to the nuclei). **M-O** – Tetranuclear embryo sac (arrows point to the nuclei) (M is pieced together by N-O, which are consecutive sections of the same embryo sac). **P-T** – 8-nucleate embryo sac (arrows) (P is pieced together by Q-T, which are consecutive sections of the same embryo sac). **AC** – antipodal cells; **EC** – egg cell; **PN** – polar nuclei; **S** – synergids.

gotene, pachytene, diplotene and diakinesis (Fig. 3D-E, Fig. 4D-F). Afterwards, the nuclear membrane disintegrates and the cell undergoes meiotic metaphase I, where homologous chromosomes are paired and arranged in the central equatorial plate (Fig. 3F, Fig. 4G). The cell undergoes meiotic anaphase I and telophase I, forming a dyad (Fig. 3G, Fig. 4H). Next, the megasporocyte undergoes a second meiosis, including prophase II, metaphase II, anaphase II and telophase II, eventually forming a tetrad (Fig. 3H, Fig. 4I) with four linearly arranged megaspores. The chalazal megaspore develops into the functional megaspore while the other three megaspores gradually disintegrate (Fig. 4J).

Female gametophyte development

The functional megaspore elongates longitudinally and moves to the center of the embryo sac, forming a mononuclear sac (Fig. 3I, Fig. 4K). The mononuclear embryo sac undergoes mitosis once and horizontally divides into a 2-nucleate embryo sac. The two nuclei initially locate in the center, then move toward the poles (Fig. 3J, Fig. 4L) and undergo mitosis once again,

forming a 4-nucleate embryo sac with two nuclei arranged on each of the two poles (Fig. 3K-M, Fig. 4M-O). Afterwards, the 4-nucleate embryo sac continues to divide, forming an 8-nucleate embryo sac. Three of the four nuclei at the micropylar end form an egg apparatus including an egg cell and two synergids, and the other nucleus becomes the upper polar nucleus. Three of the four nuclei at the chalazal end form antipodal cells and the other nucleus becomes a lower polar nucleus (Fig. 3N-S, Fig. 4P-T). At last, the upper polar nucleus moves downward, while the lower polar nucleus moves upward, and fuses together with the upper polar nucleus (Fig. 3T). The mature embryo sac has 7 cells with 8 nuclei. The embryo sac development is of the monosporic Polygonum type. Young [33] and Govil [45] found that the embryo sac development of *S. tuberosum* and *S. tuberosum* var. Jyoti Gola is of the tetrasporic Adoxa type. Overall, embryo sac development of angiosperms is monosporic, bisporic and tetrasporic, and can be further divided into 13 types [46]. The monosporic Polygonum type is the most common one, and both bisporic and tetrasporic ones are derived from the monosporic one [47-49].

Pollen morphology of *S. japonense* and *S. septemlobum*

S. japonense has very small, spheroidal pollen grains sized $8.5(7.4-9.8) \times 8.9(7.4-10.5) \mu\text{m}$. They are circular along both the polar and equatorial views, and have tricolporate and granulate-verrucate-punctate surface ornamentation (Fig. 5A-C).

S. septemlobum has very small, spheroidal pollen grains sized $8.8(7.6-9.8) \times 9.2(7.9-10.7) \mu\text{m}$. They are triangular along the polar view and circular along the equatorial view, and have tricolporate and granulate-punctate-fossula surface ornamentation (Fig. 5D-F). The pollen morphology of these two species agree with previous studies [27-29].

The colpus of pollen grains of the studied species is long, narrow and sunken, and extends almost to the poles. These features of the colpus are consistent with those of the genus *Solanum* [29]. However, the two species are different in length, width, degree of descent and the intensity of tuberculate ornamentation distributed on the surface of the colpus.

Pollen exine ornamentation is an important classification feature of Solanaceae species [29,50-52]. Our results suggest that the pollen grains of *S. japonense* have granulate-verrucate-punctate surface ornamentation, while the pollen grains of *S. septemlobum* have granulate-punctate-fossula surface ornamentation (Table 1). In addition, these species exhibit differences along the polar view. Thus, the observed details of the pollen surface can be used to distinguish between species within the genus *Solanum*.

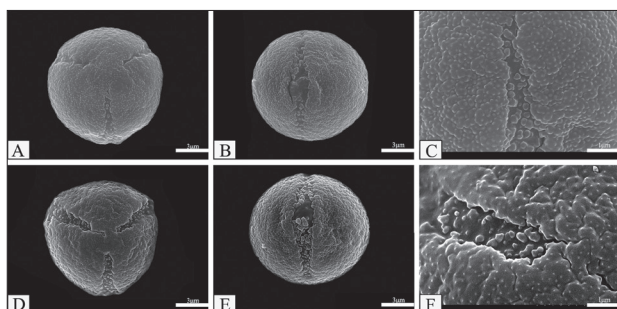


Fig. 5. SEM micrographs of pollen grains of *Solanum japonense* and *S. septemlobum*. A-C – *S. japonense*: Polar view (A); Equatorial view (B); Surface ornamentation (C). D-F – *S. septemlobum*: Polar view (D); Equatorial view (E); Surface ornamentation (F).

CONCLUSIONS

Some embryological characteristics of *S. japonense* and *S. septemlobum* were studied for the first time and their pollen morphology was also compared. The data gained from this study may contribute to the embryological and palynological characteristics used in the taxonomy of *Solanum*. Moreover, it also provides a palynological basis for the classification of these two species and a theoretical basis for their identification in TCM.

Funding: This work was supported by the National Natural Science Foundation of China (Grant No. 31270276, 30470106).

Author contributions: LYS, GL and LJX conceived and designed the experiments, contributed to the reagents, materials and analysis tools, and wrote the paper. LYS performed the experiments and analyzed the data.

Conflict of interest disclosure: The authors state that there is no conflict of interest regarding the publication of this article.

REFERENCES

1. APG IV. An update of the Angiosperm Phylogeny Group classification for the orders and families of flowering plants: APG IV. Bot J Linn Soc. 2016;181(1):1-20.
2. Bohs L. Major clades in *Solanum* based on *ndhF* sequence data. Monog Syst Botan. 2005;104:27-50.
3. Zhang ZY, Lu AM, D'Arcy WG. Solanaceae. In: Wu ZY, Raven PH, editors. Flora of China. Vol. 17. Beijing: Science Press; 1994. p. 300-32. Co-published by St. Louis: Missouri Botanical Garden Press.
4. Weese TL, Bohs L. A three-gene phylogeny of the genus *Solanum* (Solanaceae). Syst Bot. 2007;32(2):445-63.
5. Lu YY, Luo JG, Kong LY. Steroidal alkaloid saponins and steroidal saponins from *Solanum surattense*. Phytochemistry. 2011;72(7):668-73.
6. El-Hawary SS, Mohammed R, AbouZid SF, Rateb ME, Sayed AM. Cytotoxicity of *Solanum nigrum* L. green fruits on breast (MCF-7) and liver (HepG-2) cancer cell lines. Pharma Innov J. 2015;3(11):87-9.
7. Kuang KR, Lu AM. Solanaceae. In: Anonymous, editors. Flora Reipublicae Popularis Sinicae. Beijing: Science Press; 1978. p. 1-160.
8. Hunan academy of Chinese medicine. Hunan Medicine Sinicae (Third series). Changsha: Hunan People's Publishers; 1979. 388 p.
9. D'Arcy WG. Solanaceae studies II: typification of subdivisions of *Solanum*. Ann Mo Bot Gard. 1972;59(2):262-78.
10. Zhang L, Li GS, Yao F, Yue XD, Dai SJ. Three new sesquiterpenoids from *Solanum septemlobum* with cytotoxic activities. Phytochem Lett. 2015;11:173-6.
11. Zhang L, Lin HQ, Li GS, Yue XD, Dai SJ. New sesquiterpenoid derivatives from *Solanum septemlobum* with cytotoxicities. Nat Prod Res. 2015;29(20):1889-93.

12. Xie G, Duan WD, Tao BQ, Li C. Chemical constituents of *Solanum septemlobum* Bunge. *Nat Prod Res Dev*. 2008;20(4):627-9.
13. Qi ZS, Yang HS. Correction of original plants of *Solanum lyratum* Thunb. and Shuyangquan. *J Chin Med Mater*. 2001;24(7):516-7.
14. Qi ZS. A further discussion of the original plant Shuyangquan. *J Chin Med Mater*. 2002;25(9):668-9.
15. Lu AM, Wang ML. On the identification of the original plants in the modernization of Chinese herbal medicine—An example from the taxonomy and exploitation of “Gouqi”. *Acta Bot Boreal-Occid Sin*. 2003;23(7):1077-83.
16. Chen XM, Chen QH. Chinese medicine *Solanum lyratum* Thunb. and its confused species. *J Chin Med Mater*. 2005;28(6):462-3.
17. Dnyansagar VR, Cooper DC. Development of the seed of *Solanum phureja*. *Am J Bot*. 1960;47(3):176-86.
18. Siddiqui SP, Siddiqui SA. The development of endosperm, embryo and seed in *Solanum douglasii* Dunal. *B Soc Bot Fr-Lett*. 1985;132(3):233-9.
19. Kopcín J, Lotocka B, Kowalczyk K, Kobryn J. Seed development in *Solanum muricatum* Aiton. *Acta Biol Cracov Bot*. 2004;46:121-32.
20. Solís VA, Cabrera VA, Dottori N, Cosa MT. Development of fruit and seed in *Solanum argentinum* (Solanaceae). *Arnaldoa*. 2011;18(1):47-55.
21. Bhandari NN, Sharma M. Histochemical and ultrastructural studies during anther development in *Solanum nigrum* Linn. I. Early ontogeny. *Phytomorphology*. 1987;37:249-60.
22. Briggs CL. A light and electron microscope study of the mature central cell and egg apparatus of *Solanum nigrum* L. (Solanaceae). *Int J Plant Sci*. 1992;153:40-48.
23. Briggs CL. Endosperm development in *Solanum nigrum* L. formation and distribution of lipid bodies. *Ann Bot*. 1993;72(4):295-301.
24. Briggs CL. Endosperm development in *Solanum nigrum* L. formation of the zone of separation and secretion. *Ann Bot*. 1993;72(4):303-13.
25. Briggs CL. The initiation, development and removal of embryo sac wall ingrowths in the developing seeds of *Solanum nigrum* L. an ultrastructural study. *Ann Bot*. 1995;76(4):429-39.
26. Briggs CL. An ultrastructural study of the embryo/endosperm interface in the developing seeds of *Solanum nigrum* L. zygote to mid torpedo stage. *Ann Bot*. 1996;78(3):295-304.
27. Luo JS, Zhou ZZ. Pollen morphology in the watershed region of the Dabie Mountains, Anhui Province. *Acta Micropalaeontol Sin*. 2012;29(1):99-120.
28. Wang FX, Qian NF, Zhang YL, Yang HQ. *Pollen Morphology of Plants in China*. Beijing: Science Press; 1997. 461 p.
29. Du TT, Zhao CH, Liu JX. The pollen of *Solanum* L. and its systematic significance. *Palynology*. 2017; <http://dx.doi.org/10.1080/01916122.2017.1346527>.
30. Li ZL. *The Technology of Making Sections in Plant Tissues*. Beijing: Science Press; 1978. 140 p.
31. Erdtman G. *Handbook of Palynology—An Introduction to the Study of Pollen Grains and Spores*. Copenhagen: Munksgaard; 1969. 486 p.
32. Punt W, Hoen PP, Blackmore S, Nilsson S, Le Thomas A. Glossary of pollen and spore terminology. *Rev Palaeobot Palyno*. 2007;143(1-2):1-81.
33. Young WJ. The formation and degeneration of germ cells in the potato. *Am J Bot*. 1923;10(6):325-35.
34. Davis GL. *Systematic Embryology of the Angiosperms*. New York: John Wiley Press; 1966. 528 p.
35. García CC. Anther wall formation in Solanaceae species. *Ann Bot*. 2002;90(6):701-6.
36. Gui MZ. Preliminary study on the structure and the dehiscence way of anthers in several species of Solanaceae. *Journal of Northeast Agricultural College*. 1987;18(3):233-44.
37. Tian HQ. The embryogeny and the development of endosperm of *Lycium Barbarum* L.. *J Wuhan Bot Res*. 1988;5(1):17-22.
38. Wang YL, Ni XL, Tian Y, Wang JX, Chang HY, Qin BB. Microsporogenesis and development of male gametophyte of *Lycium barbarum* L. NQ-2. *Northern Horticulture*. 2011;35(4):143-5.
39. Shen JH, Li W, Yang H, Ding JT, Li RL. Studies on the megasporogenesis, microsporogenesis and development of female and male gametophyte of *Capsicum annuum* L. *Acta Hort Sin*. 2007;34(6):1443-52.
40. Ghimire B, Heo K. Embryology of *Withania somnifera* (L.) Dunal (Solanaceae). *Acta Biol Cracov Bot*. 2012;54(2):69-78.
41. Fukuda Y. Cytological studies on the development of the pollen-grain in different races of *Solanum tuberosum* L., with special reference to sterility. *Shokubutudugaku Zasshi*. 1927;41:459-74.
42. Pavari F. Ricerche Embriologiche e Cariologiche su *Cestrum Elegans* L. (Solanaceae). *Caryologia*. 1957;9(3):436-52.
43. Lengel PA. Development of the pollen and the embryo sac in *Capsicum frutescens* L. var. Japanese Variegated Ornamental. *Ohio J Sci*. 1960;60:8-12.
44. Tang HY, Cun QX, Han CK, Yan SQ, Wang Q, Liu WD. Pollen mother cell meiosis and male gametophyte development of *Solanum melongena* L. in fluorescence staining. *Jiangsu Agri Sci*. 2014;42(2):107-9.
45. Govil CM. Embryo sac development in *Solanum tuberosum* var. Jyoti Gola. *Acta Bot Indica*. 1980;8(2):263-4.
46. Willemse MTM, Van Went JL. The female gametophyte. In: Johri BM, editor. *Embryology of Angiosperms*. Berlin: Springer; 1984. p. 159-96.
47. Li L, Liang HX, Peng H, Lei LG. Sporogenesis and gametogenesis in *Sladenia* and their systematic implication. *Bot J Linn Soc*. 2003;143(3):305-14.
48. Hu SY. *Reproductive Biology of Angiosperms*. Beijing: Higher Education Press; 2005. 286 p.
49. Zhang D, Wang L, Zhuo LH. Embryology of *Iris mandshurica* Maxim. (Iridaceae) and its systematic relationships. *Plant Syst Evol*. 2011;293(1):43-52.
50. Edmonds JM. Pollen morphology of *Solanum* L. section *Solanum*. *Bot J Linn Soc*. 1984;88(3):237-51.
51. Hayrapetyan AM, Gabrielian ET. Features of the exine ornamentation of pollen grains in the family Solanaceae JUSS. I. the simple types of ornamentation. *Electron J Nat Sci*. 2008;2(11):46-50.
52. Zhang ZY, Yang DZ, Li LQ. Supplemental study on the pollen morphology of the tribe Hyoscyameae (Solanaceae) and its systematic significance. *Guihaia*. 2009;29(3):285-95.